A Digital Feedback Damping Scheme for a Micromachined Directional Microphone

N. Eva Wu†, Ronald N. Miles‡, and Oguz A. Aydin†
†Dept. of Electrical and Computer Engineering and ‡Dept. of Mechanical Engineering
State University of New York, Binghamton, NY 13902-6000
evawu,miles,oaydin@binghamton.edu

Abstract

In this paper, a method for introducing active damping for a diaphragm in a micromachined directional microphone is considered. The sigma-delta modulation is used to circumvent the nonlinearity of the capacitive transducers of the microphone. The principle of operation of the damping scheme is explained, and the simulation results of a lumped diaphragm model are presented.

1 Introduction

The system under consideration in this paper is a directional microphone consisting of a hinged conductive diaphragm (about 1mm×2mm in area, and $4 \sim 5\mu$m in thickness) that moves in response to sound pressure, and two electrically mutually isolated backplates acting as electrodes that lie side by side and are separated from the diaphragm by a small gap (about 5μm)[11,15]. Figure 1 shows the cross-section view of the lumped-mass mechanical model of the microphone that contains only its lowest resonance mode. This mode consists of pure rocking of the diaphragm about its central pivot and is excited by the difference in sound pressure acting on either side of the central pivot. The acoustic response of this pressure-difference microphone diaphragm has the figure-eight shaped directivity pattern of a first-order pressure gradient microphone. Fabricated devices have been shown to have this resonance somewhere between 2.5KHz and 3.5KHz, depending on the thickness of the diaphragm, and the next lowest resonance always occurs beyond the highest frequency (24KHz) of our interest. The microphone configuration forms two parallel plate capacitors. The microphone is therefore classified as a capacitive microphone. This microphone will be called *the* microphone or the plant to distinguish it from any other microphones.

In a conventional capacitive microphone, a single backplate serves to sense the motion of the diaphragm so that the sensed voltage can be further processed electronically. In addition, due to the small air-filled gap between the diaphragm and the backplate, viscous damping can have a significant influence on the response. In this configuration, electronic noise associated with the capacitive sensing and Brownian motion associated with the passive damping both degrade the achievable acoustic performance of the microphone in terms of SNR (Signal to Noise Ratio)[5]. In our microphone design, the two backplates are specially designed to produce little passive damping effect in order to reduce the Brownian motion, while an optical sensing scheme replaces the capacitive sensing to provide diaphragm motion readout with less thermal noise. The capacitive couplings between the diaphragm and the backplates remain to play the role of voltage-to-force transducers through which feedback control voltages could be applied to possibly damp out the resonance peak of the rocking mode. Our premise is that by careful design of the active damping system, one can achieve the desired amount of damping with less overall system noise than when passive damping is used. The rest of the paper reports our pursuit of such a possibility.

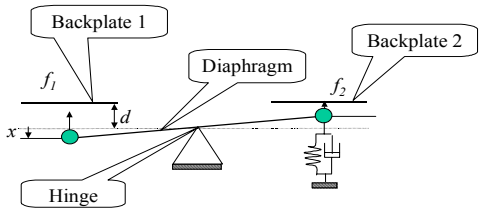

Figure 1 A lumped-mass model of a rocking diaphragm

The paper is organized as follows. Section 2 formulates the damping problem as a digital feedback control problem where the digital signal is pulse density modulated. Section 3 discusses the control design and the

demodulator design. Section 4 presents the design and simulation performed for a lumped diaphragm model. Section 5 concludes the paper.

2 Sigma-delta control loop

Figure 2 shows the schematic we propose to achieve the damping of the diaphragm rocking mode. It is anticipated that two optical diffraction grating sensors[7] will be used to measure the displacement of the diaphragm on either side of the diaphragm hinge. The difference of the two measured signals is integrated, compensated, and sampled at a very high rate. The sampled signal is fed into a one-bit quantizer (signum) followed by a one-bit digital-to-analog converter to produce a pulse-width-modulated voltage feedback. The feedback signal energizes alternately the two backplates, one at a time through one of the two nonlinear switches, to generate two force feedback signals, each of which then pulls on the corresponding side of the diaphragm to affect the damping.

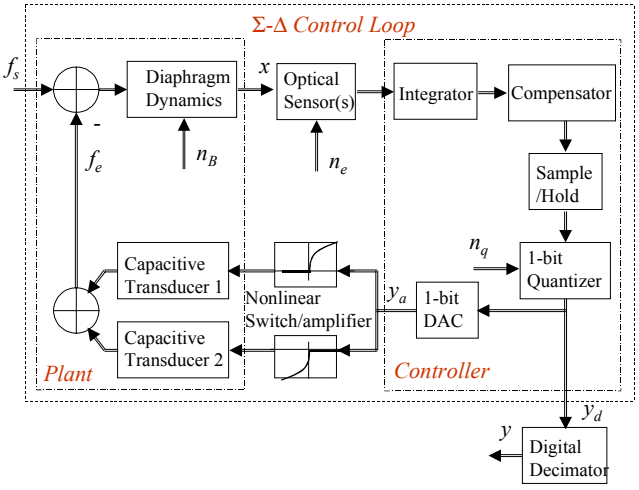

Figure 2 A directional microphone embedded in a sigma-delta modulator loop

In Figure 2, f_s and f_e are the forces exerted onto the diaphragm due to the sound pressure and the voltage applied to the capacitive transducers, respectively. Note that at the optical sensor output is the difference of the two sensor signals. n_B, n_e, and n_q are noise signals associated with the Brownian motion, the sensor noise, and the quantization error of the quantizer, respectively. y_d is the output of the control loop in the form of a pulse density modulated bit stream. y is the demodulated version of y_d which is put through low-pass filtering and down-sampling to the Nyquist rate of signal f_s. On the other hand, the DAC output is bipolar and pulse width modulated, which then passes through the two switches to become two unipolar outputs with complementary polarities. (The switches can be implemented using a pair of cascaded complementary CMOS inverters.)

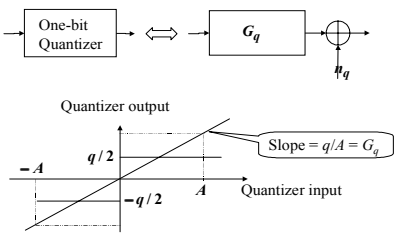

Figure 3 Linear representation of a non-overloading quantizer and quantization noise

n_B and n_e will be ignored in the following development because of their significant reduction due to our modification in backplate design and in sensing. It is well known that a wide range of damping values can be achieved through the proper selection of the distance between the diaphragm and the backplate and by the use of perforations in the backplate[14]. The quantization error (noise) captures the nonlinearity in the quantizer, and can be regarded as an additive signal at the output of a quantization gain block, as shown in Figure 3. The noise can be thought of as having a maximum magnitude of a half of quantization size q. Therefore, when the input magnitude to the quantizer exceeds A, noise level increases beyond the maximum quantization error, and the quantizer is said to be overloaded or saturated. On the other hand, since the quantizer is of one-bit, the only factor that constains its gain is the closed-loop stability.

Let us imagine that only the integrator block, the sample block, the quantizer block, and the DAC block are retained within the loop. The plant, the trasducer, the switches, the sensor, and the compensator are all identity mappings. The control loop is then reduced to a standard first order sigma-delta modulator[2]. A sigma-delta modulator is a popular quantization mechanism that can achieve high resolution with low accuracy circuitry at the expense of oversampling the integrated tracking error. It is not difficult to see that, at output y_d, the contribution from the seemingly significant quantization noise of the one-bit quantizer has been high-pass filtered, while the contribution from signal f_s has been low-pass filtered. Oversampling helps separate the pass-bands of the two filters in the digital

frequency domain. The decimator demodulates y_d to produce y. It selects the in-band portion of y_d and down-samples it to the Nyquist rate of f_s. The reader is referred to Candy and Temes[2] for a more thorough but less control-oriented discussion.

The feedback loop in Figure 2 is to be called a sigma-delta control loop because it is obtained by embedding a plant with its inherent transducer, a sensor, a pair of nonlinear switches, and a compensator in a sigma-delta modulator. Although the demodulated output of a standard sigma-delta modulator can faithfully follow its input, our imbedded system may significantly change the nature of the modulator because it contains a microphone that must be designed to satisfy some basic acoustic properties, and therefore can impose various limitations on how well the sigma-delta control loop can behave in terms of the damping performance. Our damping objective will inevitably introduce a compensator, which will further change the appearance of the sigma-delta modulator.

The most prominent reason that a sigma-delta loop is used for the feedback damping of resonance is the nonlinearity in the transducers. The nonlinearity represents a mapping from a voltage to a force proportional to the square of the voltage. The nonlinear switches split the bipolar pulse width modulated DAC output into two channels of unipolar signals. In this case, the voltage to force mapping in each channel occurs only at a single point. Therefore the nonlinearity has been circumvented.

The idea of dealing with nonlinearity by converting a sensed external signal into a binary form while encoding the information of the signal into the density of a pulse train has been successfully used in a closed-loop digital accelerometer[9,10], where the seismic mass is embedded in a sigma-delta modulation loop and a PI (proportional integral) controller is formed using the design-by-analysis approach. We are applying this idea to a different system with two unique problems.

- Above all the benefits one can expect from a closed-loop setting, our main goal is to flatten the sharp resonance peak of the microphone frequency response caused by the rocking mode of the diaphragm.
- The processing efficiency is the center of our attention because the maximum frequency f_0 of the signals our microphone is required to cope with is two orders of magnitude higher than that in the digital accelerometer[9,10], which drives the oversampling rate to MHz range, close to the limit of the current hardware (CMOS) technology for bitstream processing[1].

3 Compensator and demodulator

With the effective linearization of the quantizer and the transducers, the sigma-delta control loop can be treated as a sampled data linear system, which greatly simplifies the compensator synthesis. Our intention is to implement the compensator in the continuous domain. This is because the sigma-delta control loop is expected to have high tolerance to inaccuracy in the analog compensator, and oversampling places a high processing burden on any dynamic digital components within the sigma-delta control loop. Therefore, our analysis of this sampled data system will also be performed in the continuous domain. The only parameter that needs to be designed by emulation[6] is the quantizer gain G_q which remains the same in both the continuous and the discrete time domains.

Referring to Figure 2, y_a can be expressed in terms of n_q and f_s in the following form.

$$y_a(s) = \frac{G_a}{1+L(s)} n_q(s) + \frac{L(s)}{(1+L(s))G_f} f_s(s) \quad (1)$$

$$= H_q(s) n_q(s) + H_s(s) f_s(s). \quad (2)$$

In (1), $L(s) = G_a G_q C_I(s) P_s G_f$ is the loop transfer function of the sigma-delta control loop, where $P_s(s)$ is the plant transfer function with the optical sensor gain absorbed into it, $C_I(s)$ is the compensator with the integrator absorbed into it, G_q is the quantizer gain, and G_a is the DAC gain, G_f is the collective gain of the one of the switches/amplifiers pairs and the corresponding transducer.

If the plant model is stable and minimum phase, many classical design techniques can apply, such as loop shaping[3]. For example, a notch filter tuned to the resonance can be designed to provide a desired loop shape — a high loop gain at the low frequency and the same roll off rate as the plant at the high frequency. Once $C_I(s)$ has been designed and all the gains have been selected, H_q and H_s can be explicitly obtained. In this case the output SNR is

$$SNR = \frac{P_{signal}}{P_{noise}} = \frac{\int_{-f_0}^{f_0} |H_s(j2\pi f) f_s(j2\pi f)|^2 df}{\int_{-f_0}^{f_0} |H_q(j2\pi f)|^2 S_q(2\pi f) df} \quad (3)$$

where $S_q(\omega)$ is the power spectral density of the quantization noise, P_{signal} is the output signal power, P_{noise}

is the contribution of the total output noise to the signal band, and f_0 is 24KHz in our application. In the next section, a compensator design is carried out for an experimentally identified nominal model of a directional microphone. Note that the above convenience in compensator design is easily lost once practical factors, such as overloading and model uncertainty, are taken into consideration. We are working currently to address these practical problems.

What should be the appropriate oversampling rate f_{os} in order to achieve the required fidelity in y_a or in y? It is seen from (3) that the answer requires the knowledge of all the transfer functions in the loop. Therefore, the oversampling rate is not a quantity that can be determined before the compensator is designed. An estimate can be obtained, however, from a slightly modified existing result[1] by assuming a standard sigma-delta loop,

$$f_{os} \approx SNR_y \frac{2\pi f_0}{\sqrt[3]{3\pi}} \sqrt[3]{\frac{ms_q^2}{ms_s^2}} \tag{4}$$

Let us turn to the problem of demodulating the pulse density modulated y_d. What is expected from the microphone output y is a digital version of f_s sampled at its Nyquist rate so that it can be efficiently further processed. In principle, demodulation can be accomplished by a low-pass anti-aliasing filter, followed by a down-sample of $OSR = f_{os}/(2f_0)$ times. Since the low-pass filter must be operated at the oversampling rate, a filter performance requirement such as a sufficiently sharp transition from pass-band to stop-band could drive up significantly the processing requirement. Our ultimate goal is to integrate the diaphragm with its transducer, sensor, compensator, switches and amplifiers, clocked sampler and quantizer, DAC, and all the filters into one system-on-chip, and manufacture the system using bulk technology at low cost. Therefore, minimizing the processing requirement is an important consideration in our design.

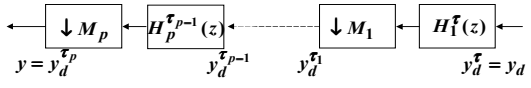

Figure 4 Demodulation using multistage filtering and decimation

It is possible that a multiple stage filter/decimation process is more computationally efficient than a single stage[12]. The number of stages and the down-sample rate at each stage are determined by how well the selected configuration can lead to a minimized overall processing requirement. The benefit mainly comes with a more relaxed filter transition band requirement in the earlier stages when the sampling rates are still high. Figure 4 depicts a p-stage decimator. The superscript of a symbol denotes the sampling interval of the corresponding discrete-time signal/system in real-time. In particular, $\tau = 1/f_{os}$ is the oversampling interval, M_i is an integer denoting the decimation ($\downarrow$) factor[12] at the ith stage, and p is constrained to

$$2 \times f_0 \le \frac{f_{os}}{M_1 \times M_2 \cdots \times M_p},\ \tau_i = \prod_{k=1}^{i} M_k \tau, \tag{5}$$

The selection of M_i and p is an optimization problem solvable by exhaustive search. There are some guidelines in the literature[12]. For example, if a finite impulse response (FIR) filter is to be designed at the ith decimation stage using a Kaiser window with stop-band and pass-band magnitude tolerance at $\delta_{s,i}$ and $\delta_{p,i}$, respectively, and stop-band and pass-band cutoff at $\theta_{s,i}$ and $\theta_{p,i}$, respectively, the order of the filter N_i can be estimated using Kaiser's empirical formula

$$N_i = \frac{-20\log_{10}\sqrt{\delta_{p,i}\delta_{s,i}} - 13}{2.32|\theta_{p,i} - \theta_{s,i}|}. \tag{6}$$

The computational complexity ξ_i at the ith decimation stage can be estimated by the number of multiplications the filter must perform for each input sample, which leads to

$$\xi_i = \frac{N_i + 1}{M_1 \times \cdots \times M_i}. \tag{7}$$

The complexity measure is used in the next section to help determine the decimator configuration in our example.

4 Active damping of a lumped model

The following transfer function for a diaphragm is experimentally identified using a scanning laser vibrometer.

$$P(s) = \frac{2.64 \times 10^8}{s^2 + 321.6s + 2.585 \times 10^8}.$$

This model contains two lightly damped poles with damping ratio $\xi = 0.01$, representing a rocking mode at $f = 2.559$KHz. We take the approach of starting from a desirable closed-loop transfer function

$$T(s) = \frac{1.5^2 \times 10^{10}}{s^2 + 2 \times 0.95 \times 1.5 \times 10^5 s + 1.5^2 \times 10^{10}},$$

with a damping ratio 0.95, and working backwards to solve for the compensator

$$C_I(s) = \frac{56.8 \times (s^2 + 321.6s + 2.585 \times 10^8)}{s(s + 2.85 \times 10^5)}.$$

Note that this compensator contains all the gains around the loop. Also a pole-zero cancelation occurs between P_s and C_I. Therefore, this method will not work for nonminimum phase or unstable plant models. If there is some uncertainty about where the resonance occurs, a more prudent approach is to slightly increase the number 321.6 in the numerator. This would produce a shallower but wider notch[3].

Using (4), the required oversampling rate for an active damping scheme using sigma-delta modulation (Figure 2) is estimated at 5MHz. A third order IIR (Infinite Impulse Response) filter

$$H_1^\tau(z) = \frac{0.0440z^2 + 0.1721z + 0.0421}{z^3 - 2.9113z^2 + 2.8253z - 0.9139}.$$

with a decimator of down sample factor ⇃100 is used to perform demodulation. The above compensator and demodulator designs are used to damp the 2.559KHz rocking mode of our plant. A test speech signal created using the modulation demo file mtlb.mat from MATLAB Signal Processing Toolbox is applied to the closed-loop microphone. Various responses are plotted in Figure 5 and Figure 6. The Simulink[16,4] diagram of the closed-loop microphone with IIR/decimation demodulation is shown in Figure 7.

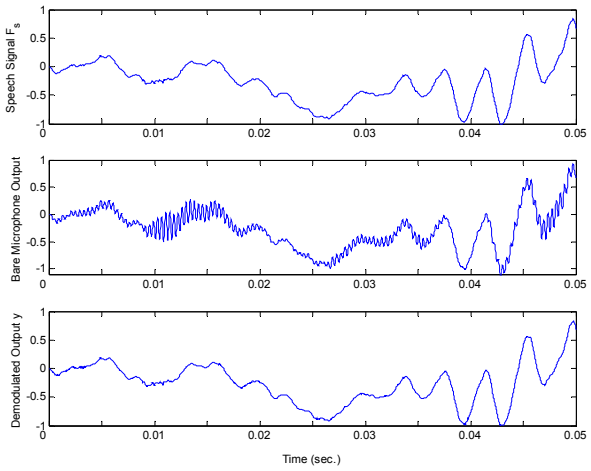

Figure 5 The first 0.05 seconds of a speech signal, the output of the microphone without the active damping, and the demodulated speech signal sampled at 50KHz from the output of our sigma-delta control loop.

In Figure 5 the oscillation at the diaphragm resonance frequency when the microphone is not compensated is clearly visible. The plots in Figure 6 are 100 times decimated and zoomed in for easy viewing.

Because of the implementation concern, attempts are also made on multistage FIR filtering/decimation. The Table 1 summarizes the computational complexity estiamte using (6) and (7)

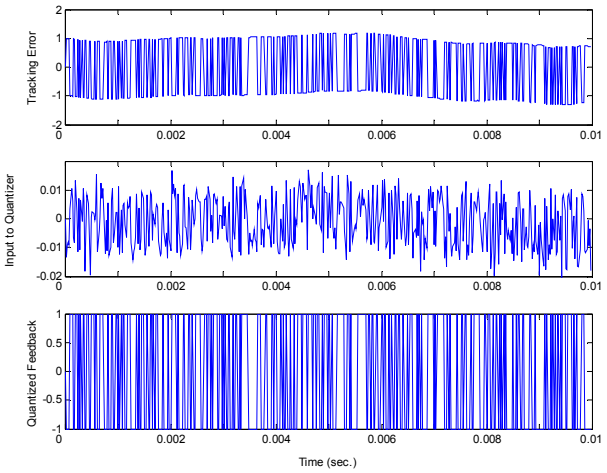

Figure 6 Tracking error, quantizer input, quantized feedback force signals in the sigma-delta control loop sampled at $f_s = 5$MHz.

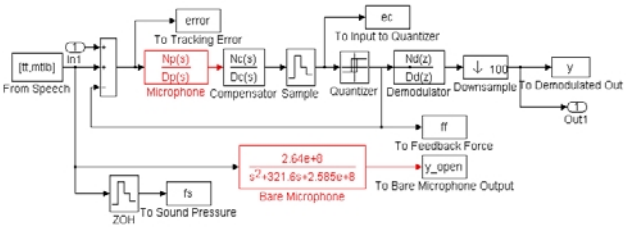

Figure 7 Simulink diagram for closed-loop simulation

Stage i	Stage 1	Stage 2	Stage 3	Complexity
(N_i, ξ_i)	(N_1, ξ_1)	(N_2, ξ_2)	(N_3, ξ_3)	$\sum \xi_i$
$5 \times 5 \times 4$	$(8, 1.8)$	$(22, 0.92)$	$(300, 3.01)$	5.73
$10 \times 5 \times 2$	$(17, 1.8)$	$(749, 15)$	$(150, 1.51)$	18.31
10×10	$(16, 1.7)$	$(687, 6.88)$	N/A	8.58

Table 1 Complexity estimation in terms of total number of multiplications per input sample ($\delta_{p,i} = 0.033$ and $\delta_{s,i} = 0.01$)

It is apparent the factorization that leads to the least computational complexity is

$$M = M_1 \times M_2 \times M_3 = 5 \times 5 \times 4.$$

The three stages of filters are designed with the passband, stopband cutoff frequencies (radians/sample), and passband and stop band ripple specified as follows.

Stage i	Stage 1	Stage 2	Stage 3
$(\theta_{p,i}, \theta_{s,i})$	$(.0096\pi, .39\pi)$	$(.048\pi, .19\pi)$	$(.24\pi, .25\pi)$
$(\delta_{p,i}, \delta_{s,i})$	$(.033, .01)$	$(.033, .01)$	$(.033, .01)$

Table 2 Multistage filter specifications

The filters are implemented using FIR decimation blocks provided by the Matlab DSP Blockset[4], and using polyphase decimation filters[12]. The hardware and realtime implications of the IIR and the FIR implementations are being investigated.

The demodulated signals with different decimation filters are tested using the MATLAB demo program for their receptability by ears. All cases are indistinguishable with respect to the re-sampled original signal (mtlb.mat). It is found that even with the stop-band tolerance increased to $\delta_{s,i} = 0.1$ (10 time worse than the situation in Table 1 with almost a half of the complexity in all three configurations), the 3-stage demodulated signal still sounds good.

5 Conclusions

This paper proposes a digital active damping scheme for a micromachined directional microphone where a rocking mode of the diaphragm associated with the directivity of the microphone occurs in the audible range. The feedback loop is a sigma-delta modulator with a notch filter embedded as a dynamic compensator. The loop closure is fulfilled by two optical diffraction grating sensors and two capacitive transducers inherent to the microphone structure. The proposed scheme was analyzed and realized in Simulink[16] for an experimentally identified lumped diaphragm model. The simulation results show that the active damping scheme is feasible. Answers are being sought for many practical questions that are still open with regard to experimental modeling and testing, realization of dynamic compensation, circuit design and integration, analysis of noise performance, and micro-fabrication of the microphone.

6 Acknowledgment

The first author would like to express her sincere thanks to Professor Mark Fowler of the Department of Electrical Engineering at Binghamton University for giving her a set of most excellent lectures on multirate filtering.

References

[1] Aziz, Sorensen, and van der Spiegel, An overview of sigma-delta converters, *IEEE Signal Processing Magazine*, pp.61-84, Jan., 1996.

[2] Candy, J. C., Temes, G.C., editors, *Oversampling Delta-Sigma Data Converters: Theory, Design, and Simulation*, IEEE Press, 1992.

[3] Doyle, J.C., Frances, B.A., and Tannenbaum, A.R., *Feedback Control Theory*, Macmillan Publishing Company, 1992.

[4] *DSP Blockset User's Guide*, (Dynamic System Simulation for *MATLAB*), The MathWorks, 2002.

[5] Gabrielson, T., Mechanical-thermal noise in micromachined acoustic and vibration sensors, *IEEE Transactions on Electron Devices*, vol.40 pp.903-909, 1993.

[6] Franklin, G.F., Powell, J.D., and Workman, M.L., *Digital Control of Dynamic Systems*, 3rd ed., Addison-Wesley, 1997.

[7] Hall N.A. and Degertekin F.L., An integrated optical interferometric detection method for micromachined capacitive acoustic transducers, *Appl. Phys. Lett.*, vol.80, pp.3859-61, 2002.

[8] Hayes, M.H. *Statistical Digital Signal Processing and Modeling*, John Wiley & Sons, 1996.

[9] Kraft, M., *Closed Loop Digital Accelerometer Employing Oversampling Conversion*, Ph.D. Thesis, Conventry University, 1997.

[10] Lemkin, M., and Boser, B.E., A three-axis micromachined accelerometer with a CMOS position-sense interface and digital offset-trim interface, *IEEE Journal of Solid State Circuits*, vol.34, pp.457-468, 1999.

[11] Miles, R. N., Sundermurthy, S., Gibbons, C., Hoy, R., and Robert, D., Differential Microphone United States Patent application filed August 1, 2001, serial number 09/920,664, 2001.

[12] Porat, B. *A Course in Digital Signal Processing*, John Wiley & Sons, 1997.

[13] Ricketts, T.A. . Directivity quantification in hearing aids: Fitting and measurement effects, *Ear and Hearing*, vol. 21, pp.45-58, 2000.

[14] Skvor, Z . On the acoustical resistance due to viscous losses in the air gap of electrostatic transducers, *Acustica*, vol. 19, pp.295-299, 1967.

[15] Tan, L., Miles, R.N., Weinstein, M. G., Miller, R. A., Su, Q., and Cui, W. Response of a biologically inspired MEMS differential microphone diaphragm, *Proceedings of the SPIE AeroSense 2002*, Paper No. 4743-15, 2002.

[16] *Using Simulink* (Dynamic System Simulation for *MATLAB*), The MathWorks, 1999.